Solvent effects and hydration of a tripeptide in sodium halide aqueous solutions: an *in silico* study†

Maxim V. Fedorov,[a] Jonathan M. Goodman[a] and Stephan Schumm [b]

Received 1st May 2007, Accepted 9th July 2007
First published as an Advance Article on the web 31st July 2007
DOI: 10.1039/b706564g

In this work we are trying to gain insight into the mechanisms of ion–protein interactions in aqueous media at the molecular scale through fully atomistic molecular dynamics simulations. We present a systematic molecular simulation study of interactions of sodium and halide ions with a trialanine peptide in aqueous sodium halide solutions with different salts concentrations (0.20, 0.50, 1.0 and 2.0 M). Each simulation covers more than fifty nanoseconds to ensure the convergence of the results and to enable a proper determination of the tripeptide–ion interactions through the potentials of mean force. Changes in ion densities in the vicinity of different peptide groups are analysed and implications for the tripeptide conformations are discussed.

1. Introduction

Most biomolecules, whether *in vivo* or *in vitro*, function in crowded aqueous environments that contain a significant amount of dissolved salts. It has long been known that salts can significantly affect structural and thermodynamic properties of macromolecules.[1–3] Although salt effects on biomolecules have been well studied both theoretically[4–8] and experimentally,[9–17] the question "What are the effects of different ions and their concentrations on a macromolecular solute?" has not been completely answered yet.

Following ref. 1, 2 and 10, we note that the addition of salts has at least three major effects that may affect the macromolecular conformation:

1. Debye–Hückel screening effect on the electrostatic interactions between protein charged groups. The magnitude of this effect is determined **only** by the ionic strength of the solution.

2. Electroselectivity—specific interaction with charges by ion-pair formation (or ion binding). If this effect is dominant, the effects of different ions on the conformational properties of polypeptides/proteins should follow the *electroselectivity* series of the salts towards anion (cation)-exchange resins.[10]

3. Hofmeister effect—salts can distort water structure which consequently changes the hydrophobic interactions of proteins and biomolecules. The importance of this factor can be determined by comparing the effect of different ions with the *Hofmeister* series.[18,19] The Hofmeister series is different from the electroselectivity series. For halide anions the electroselectivity series has almost the inverse order to the Hofmeister series.

One of the most popular semiempirical theories, which attempts to generalise all these phenomena is Timasheff's theory of preferential interactions.[20] This theory proposes different mechanisms of protein–ion interactions. Some ions are preferentially excluded from the protein–water interface, increasing the surface tension of water on the interface which leads to protein precipitation and the stabilising of more compact folded states of the protein. There is also another competitive process: direct ion binding to polar side chain residues and backbone groups can change the structure of hydration shells around the polar groups that might lead to denaturation of the proteins. But at the same time, the bound ions can stabilise the macromolecule conformation through the salt bridges.[1] Therefore, ions can have a double effect on the macromolecule conformation: firstly, they can influence the macromolecule conformation in an implicit way through the changes in the water activity (amount of water available for hydration of macromolecules[21]) and, secondly, they can explicitly affect the macromolecule conformation through the direct binding.

In this article we investigate the competition between these two opposite mechanisms of ion–protein interactions by molecular simulations at the atomic resolution scale. We performed long range molecular dynamics (MD) simulations of the alanine tripeptide (AA3) in ionic solutions with a fully atomistic protein force-field and an explicit water model. We have chosen this tripeptide as a model system because it is one of the simplest examples of a biomolecule which contains the essential features of proteins. To investigate the specific effects of the halide anion series we simulated aqueous solutions of sodium salts of fluorine, chlorine, bromine and iodine with different molar concentrations: 0.20, 0.50, 1.00 and 2.00 M.

We investigated relative concentrations of ions in the vicinity of different peptide groups and compared them with bulk values for these ions. The calculated variations of ion density were related to changes in the peptide conformation. We also analyzed the interactions of ions with water and different peptide groups *via* the potentials of mean force (PMF). In the spirit of Samoilov's conception on 'positive' and 'negative' ion hydration[22,23] we characterise the activated jumps of ions and water from an immediate vicinity of the peptide groups by an activation energy which we calculated from the corresponding PMFs.

[a] *Unilever Centre for Molecular Science Informatics, Department of Chemistry, University of Cambridge, Lensfield Road, Cambridge, UK CB2 1EW*
[b] *Unilever Food and Health Research Institute, Unilever R&D Vlaardingen, Olivier van Noortlaan 120 3133 AT Vlaardingen, The Netherlands*

† Electronic supplementary information (ESI) available: Further experimental details (Fig. S1–S15). See DOI: 10.1039/b706564g

2. Materials and methods

A. Procedure for MD simulations

We used the Gromacs MD software package.[24,25] For our simulations we employed the OPLSAA-2001 fully atomistic force field.[26] In all simulations we placed the tripeptide in a periodic dodecahedron box of TIP5P-EW water.[27] Electrostatic interactions were treated with use of the particle mesh Ewald (PME) summation technique. The TIP5P-EW water is a slightly modified version of TIP5P water[28] which is optimised for PME. For simulations of bulk water solution we used 1201 water molecules in the box with the corresponding peptide concentration of 0.05 mol l^{-1}. For simulations of ionic solutions of AA3 we randomly substituted some of the water molecules by the corresponding ions to provide a finite concentration of ions. We used the following concentration range: 0.20; 0.50; 1.00 and 2.00 mol l^{-1}. In Table 1 we give the numbers of ions in the water box for each concentration. We took the ion parameters from the OPLSAA-2001 standard set of ion parameters.[26]

We generated our *in silico* model of the tripeptide using the Molden software.[29] The initial conformation of the tripeptide corresponded to a segment of an ideal alpha-helix with central (Φ, Ψ) dihedral angles equal to (-57°, -47°). We assumed that all the solutions have neutral pH (pH = 7.0) where this tripeptide is a zwitterion. Therefore, in our model we used the protonated form of the tripeptide amino terminus (NH_3^+) and the deprotonated form of the tripeptide carboxyl terminus (COO^-).

The choice of this particular combination of the OPLSAA-2001 force-field and the five-sites TIP5P-EW water model was from previous work[30] and our preliminary simulation study[31] of the tripeptide conformations in different brine solutions where it was shown that such a combination predicts conformational properties of the trialanine close to experimental results.[32–34] In addition, a comparative study of different biomolecular force-fields shows[35] that the OPLSAA force-field performs considerably better with more detailed water models than the commonly used SPC model.

The first step in the computational procedure was the minimisation of the potential energy of each system by using a version of the steepest descent algorithm.[24,25] Then, for each system, we performed a single nanosecond equilibration run with NVT conditions and constrained positions of the tripeptide atoms to equilibrate solvent molecules in the box. This was followed by a 27 ns equilibration run for the system with NPT ensemble where the pressure and the temperature were maintained at 1 atm and 300 K by coupling the system to a heat bath *via* the Berendsen thermostat.[36] Such long preliminary simulations provided a good equilibration of the system. After this we performed an additional 27 ns production run. We collected the data each 0.2 ps. For integration of Newton's equations of motion we used the velocity Verlet algorithm with a timestep of 2 fs.

For preprocessing and analysis of the MD data we mainly used the GROMACS analysis tool.[24,25] We used this collection of different programs and subroutines for calculating the solvent accessible area, dihedral angles, *etc*. We calculated the peptide solvent accessible area by the *g_sas* program from the GROMACS analysis tool, using a solvation probe of radius 1.4 Å. For further preprocessing of the results we used the OCTAVE software.[37] All pictures in this work were created using the GNUPLOT 4.0 software.[38]

Table 1 Number of ions and water molecules in the box for different salt concentrations

Concentration/M	$N_{cations}$	N_{anions}	N_{water}
Bulk	0	0	1201
0.20	4	4	1193
0.50	11	11	1179
1.00	21	21	1159
2.00	42	42	1117

B. Convergence of sampling

To check how robust our results are, we investigated the problem of how efficiently ions sample the simulation box during the available simulation time. Fig. 1 presents the part of the available volume (volume of the box without the excluded volume of the tripeptide) visited by the total number of chlorine ions as a function of simulation time. The data are shown for different concentrations of ions. It can be seen that the time needed to sample the whole volume of the simulation box decreases with increasing concentration. For low concentrations (0.50 and 0.20 M) the simulation time for 95% sampling of the available volume is quite large: $\simeq$7 and $\simeq$12 ns, respectively. This time decreases with increasing concentration but it is always of the order of nanoseconds. For other solutions we obtained very similar dependencies of the sampling time on the concentration (data not shown). Therefore, it is clear that in order to obtain converged results for salt solutions at concentrations close to physiological values (0.10–0.30 M) simulation times much greater than $\simeq$10 ns are needed.

3. Results and discussion

A. Conformation changes

For investigations of conformational changes of the tripeptide with regard to the concentration and type of anions, we use the same approach as we used in ref. 31. For all the systems we calculated the density of conformational states projected on the plane of Ramachandran angles (Φ, Ψ) of the central AA3 residual. In the case of bulk water solution, the most favoured conformation is the Poly-Proline II (PPII) conformation ($\Phi \approx -80^\circ$, $\Psi \approx 140^\circ$) (see ref. 31 and ESI†). There are additional, secondary maxima on this map which correspond to the beta-sheet and alpha-helix conformation, respectively. Such distribution is in a good correspondence with experimental results[32–34] and previous simulation study of the trialanine conformations in water.[30]

The turn and helical conformations have a smaller solvent accessible surface (SAS) than the beta-sheets and PPII conformations.[1,2,31] The result is a general consequence of the polypeptide geometry—the turn and helical conformations are more compact, and, therefore, have smaller SAS compared to 'extended' conformations.

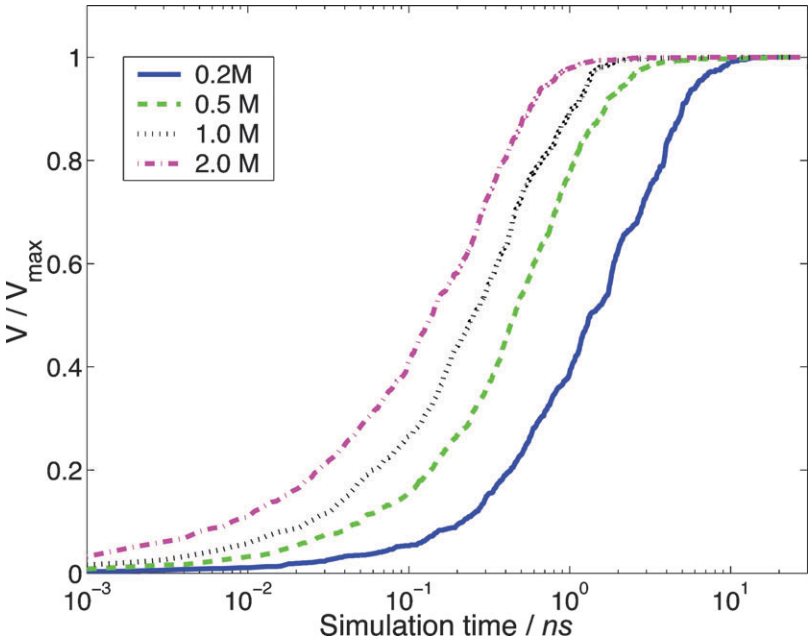

Fig. 1 The sampled fraction V of the available volume V_{av} (volume of the box without the excluded volume of the tripeptide) visited by any of the Cl^- ions as a function of simulation time. The data are shown for different concentrations of ions: solid line – 0.20 M, dashed line – 0.50 M, dotted line –1.00 M and dash dotted line corresponds to 2.00 M concentration. This figure demonstrated that equilibration times ~1–10 ns are required for Cl^- to visit every part of the simulation box.

This distribution of SAS with regard to the dihedral angles gives us a method to make a crude classification of the tripeptide conformations. Thus, to generalise the data we calculated the ratios (in percents) of 'folded' and 'extended' conformations for all investigated systems which are given in Table 2. We determine these ratios in the following way: any conformation of AA3 with (Φ, Ψ) belonging to the region ([−110°: −20°], [−70°: +50°]) we label as a 'compact' conformation. All other conformations we label as 'extended'. Of course, such separation of the density space is somewhat arbitrary but it helps to reveal the most important trends in the conformational changes of the tripeptide.

As may be seen from this table, the number of compact conformations varies with type and concentration of ions. Fluorine seems to be the best stabiliser of the compact conformation up to the solubility limit of NaF ($\simeq$1.0 M). Other salts behave differently, but the general trend corresponds to the electroselectivity hypothesis rather than the Hofmeister series. On average, the chaotropic anions (Br^- and I^-) seem to be better stabilisers than the chloride anion which possesses almost neutral kosmo-/chaotropic properties.

Table 2 % of compact ('folded') conformations of the tripeptide for different salt concentratioin. For comparison, we also give this number for bulk water solution (0.0 M salt concentration)

Salt	0.0 M	0.20 M	0.50 M	1.00 M	2.00
NaF	12.2	21.9	52.6	33.8	15.3[a]
NaCl	12.2	17.1	14.5	9.0	9.0
NaBr	12.2	19.5	16.1	21.2	14.8
NaI	12.2	22.5	15.2	20.2	10.9

[a] —the 2.0 M concentration is above maximum solubility of NaF salt.

B. Local densities

To gain insight into the tripeptide–ion interactions at the atomistic level we performed the following calculations: for each MD time-frame we calculated the number of ions N_{ions} and water molecules N_{water} in the first and second solvation shell of the whole tripeptide and its functional groups, respectively: terminal basic amino group NH_3^+; terminal acidic carboxyl COO^- group; all backbone groups and all side chain groups. As the water density profiles around polar and nonpolar groups are substantially different,[1–3] we used different geometrical limits for the first solvation shell: $R^{first}_{polar} = 3.5$ Å for the polar groups (NH_3^+, COO^- and backbone groups) and $R^{first}_{nonpolar} = 4.0$ Å for the nonpolar side chain groups. For the first solvation shell of the whole tripeptide we used geometrical limit $R^{first}_{total} = 3.5$ Å. Correspondingly, we used different geometrical limits for the second hydration shell as: $R^{second}_{total} = R^{second}_{polar} = 5.5$ Å and $R^{second}_{nonpolar} = 6.5$ Å.

After obtaining the numbers of ion and water molecules in the first and second solvation shells we calculated the relative ratios of 'local' ion concentrations in these shells with regard to the corresponding bulk concentrations. We determine these parameters n^s as:

$$n^s = \frac{N^s_{ions}}{N^s_{water}} \frac{N^{bulk}_{water}}{N^{bulk}_{ions}}, \quad (1)$$

where the N^s_{ions} and N^s_{water} are the average number of ions and water molecules in the shell s; N^{bulk}_{ions} and N^{bulk}_{water} are the corresponding values for the whole simulation box (see Table 1). As the fluoride anions have a very strong affinity to the peptide, and this is an order of magnitude higher than the affinities of the other halide ions, we show the fluoride results on separate plots in the ESI.† The results for the relative concentrations of the other halide ions in the solvation shells around the whole tripeptide are shown in Fig. 2. The results for relative concentrations of ions for solvation shells around the NH_3^+ cationic group are shown in Fig. 3. The results for relative concentrations of ions for solvation shells around the COO^- group are shown in Fig. 4. The results for relative concentrations (average values) of ions for solvation shells around the polar backbone groups are shown in Fig. 5. The results for relative concentrations (average values) of ions for solvation shells around the hydrophobic side groups are shown in Fig. 6. The data are shown for all concentrations studied (0.20, 0.50. 1.0 and 2.0 M).

As one may see from these pictures, the 'local' densities of ions have very peculiar behaviour which sometimes seems to be opposite to common sense. For solutions of the small ions we have a strange picture: the ions seem to be attracted to peptide groups of the like charge. The effect of the like charges attraction in polar liquids is described in the literature.[39–42] It happens in aqueous solutions because of the reorientation of water dipoles in the presence of electric field.[39,43] This could serve as an explanation for the failing of conventional *continuum* models in describing ion–protein interactions. In addition, for the case of sodium iodide solution, we can see that the 'local' density of iodide in the first solvation shell of the cationic terminal amino group NH_3^+ is significantly less than the density of iodide ions in the first solvation shell of the nonpolar side groups (compare Fig. 3 and Fig. 6). We suggest that this is due to the entropy gain from replacing some of the 'frozen' water molecules near the hydrophobic groups by the large iodide. Presumably, this increase of entropy (the released water molecules have more freedom) compensates for some increase in electrostatic potential energy. This conclusion is in line with the results of recent studies of hydrophobic objects in aqueous salt solutions[44–47] where it was found that decreasing the charge density of anions (by increasing their size) leads to their increasing propensity to interact favourably with hydrophobic solutes.

Similar effects can happen with hydration of backbone groups: 'local' densities of anions (except fluoride) are higher around the hydrophobic side groups than around the polar backbone groups. Moreover, for most of the cases, the 'local' densities of ions near the backbone groups are less than in the bulk solution (n^1, $n^2 < 1$). This is a consequence of geometrical constraints (the backbone groups are generally less exposed to the solvent than the side chains) and strong dipole–dipole interactions of water molecules with the backbone groups.

In addition, it appears that electrostatic interactions are dominant in the case of smaller ions—sodium, fluoride and,

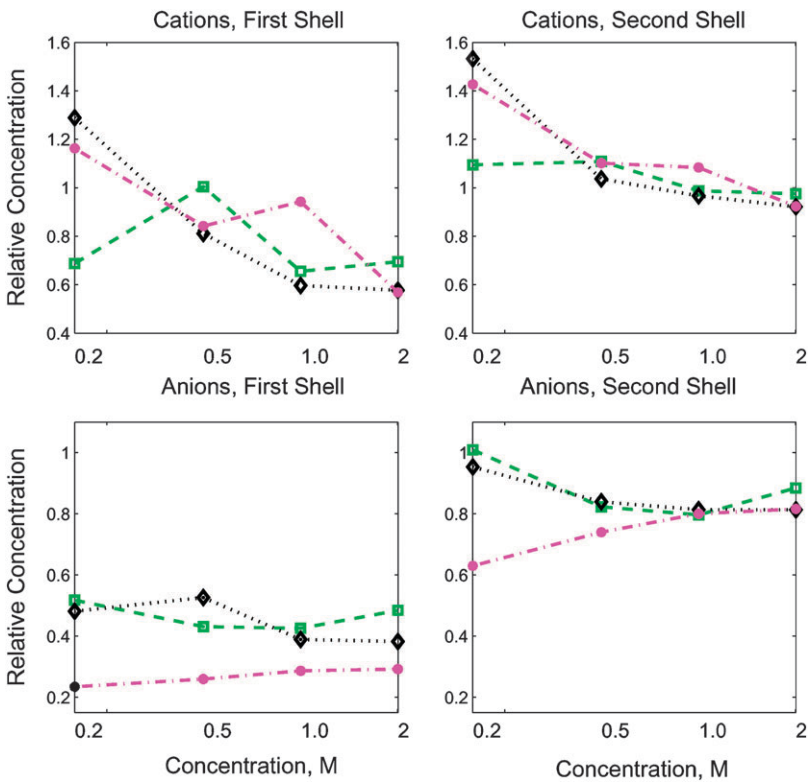

Fig. 2 Relative 'local' density of sodium cations (top) and halide anions (bottom) in the first (left) and second solvation shell of the whole tripeptide plotted against the concentration of ions. The concentrations are 0.20, 0.50, 1.00, and 2.00 M. Different lines correspond to different anions: dashed line (□) – Cl^-; dotted line (◇) – Br^-; dash-dotted line (●) – I^-.

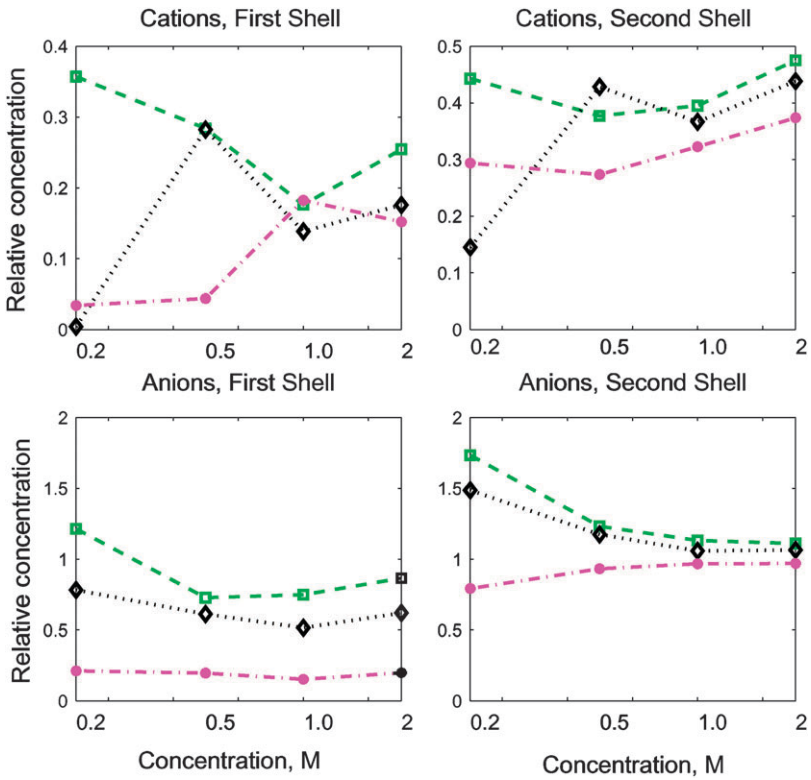

Fig. 3 Relative 'local' density of sodium cations (top) and halide anions (bottom) in the first (left) and second solvation shell of the tripeptide amino terminus (NH_3^+) plotted against the concentration of ions. The concentrations are 0.20, 0.50, 1.00 and 2.00 M. Different lines correspond to different anions: dashed line (□) – Cl^-; dotted line (◇) – Br^-; dash-dotted line (●) – I^-.

sometimes, chloride. In the case of fluoride we have very strong binding of this ion with cationic sites, which leads to a dramatic increase of the 'local' density of these anions in the close vicinity of the tripeptide. Reorientation of water dipoles by this shell of fluorides leads to an increase of the 'local' sodium concentration as well.

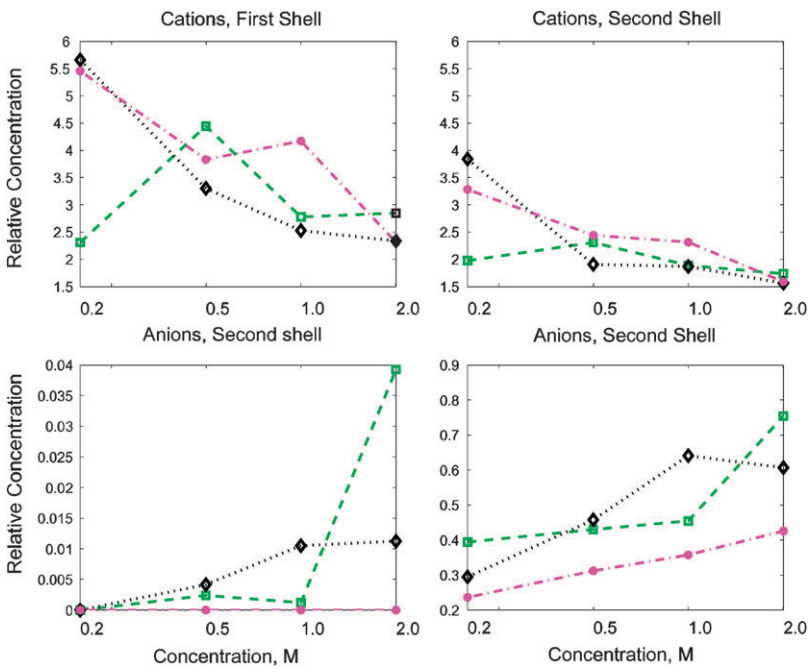

Fig. 4 Relative 'local' density of sodium cations (top) and halide anions (bottom) in the first (left) and second solvation shell of the tripeptide carboxyl terminus group (COO^-) plotted against the concentration of ions. The concentrations are 0.20, 0.50, 1.00 and 2.00 M. Different lines correspond to different anions: dashed line (□) – Cl^-; dotted line (◇) – Br^-; dash-dotted line (●) – I^-.

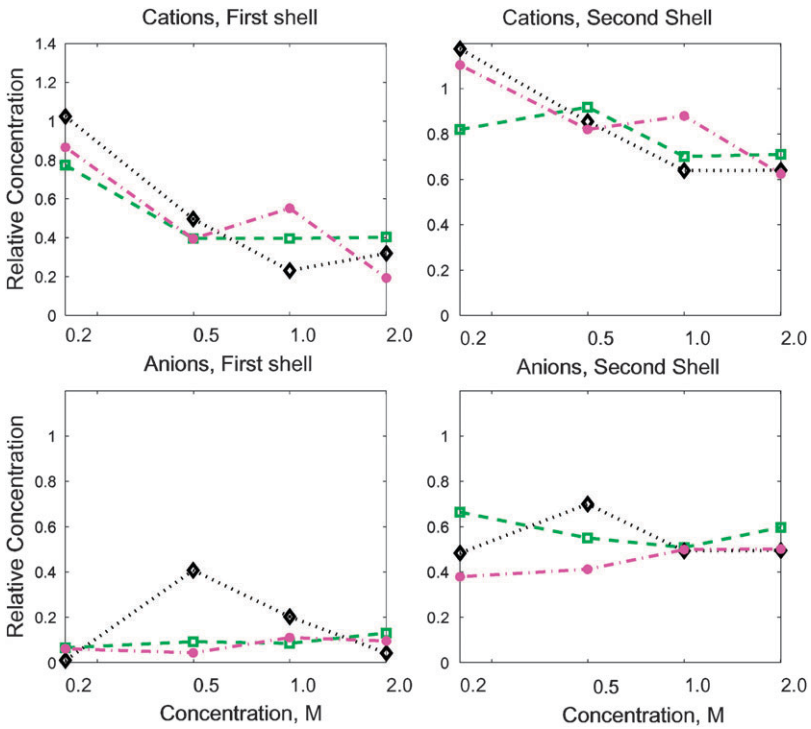

Fig. 5 Relative 'local' density of sodium cations (top) and halide anions (bottom) in the first (left) and second solvation shell of the tripeptide backbone groups plotted against the concentration of ions. The concentrations are 0.20, 0.50, 1.00 and 2.00 M. Different lines correspond to different anions: dashed line (□) – Cl^-; dotted line (◇) – Br^-; dash-dotted line (●) – I^-.

C. Potentials of mean force for different co-solutes

To reveal more details of the tripeptide–ion interactions we calculated the potentials of mean force (PMF) between the tripeptide and the co-solutes (water, anions and cations).

We determine the site–site PMFs $F_{ij}(r)$ by the classical formula:[3]

$$F_{ij}(r) = -(k_B T)\log(g_{ij}(r)) \quad (2)$$

where the $g_{ij}(r)$ is the density correlation function (DCF) for sites i and j, k_B is the Boltzmann constant and T is the

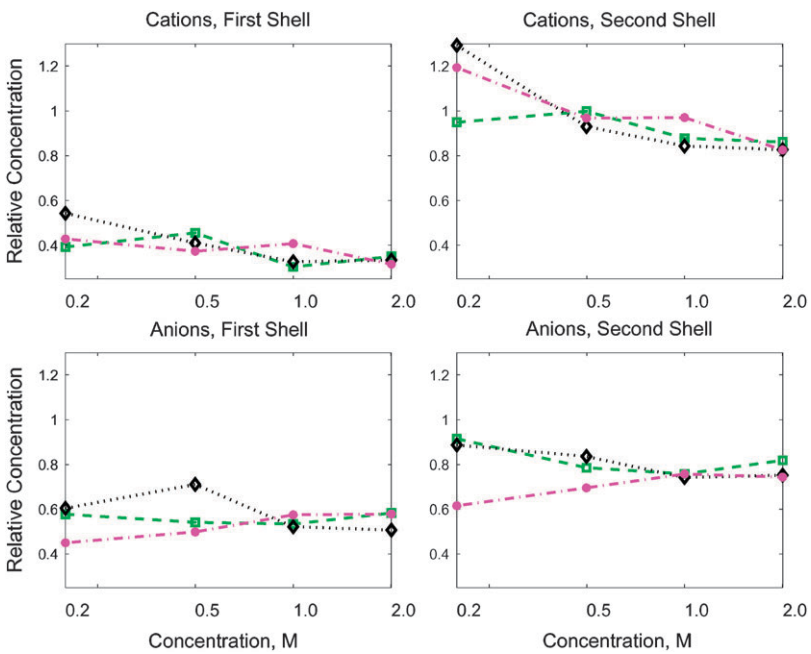

Fig. 6 Relative 'local' density of sodium cations (top) and halide anions (bottom) in the first (left) and second solvation shell of the tripeptide side groups plotted against the concentration of ions. The concentrations are 0.20, 0.50, 1.00 and 2.00 M. Different lines correspond to different anions: dashed line (□) – Cl^-; dotted line (◇) – Br^-; dash-dotted line (●) – I^-.

temperature. We use here the one-dimensional approximation of DCFs which gives us a probability of finding the site i at a distance r from the site j. This gives us an approximate picture of ion and water distributions around the tripeptide assuming that the shapes of the tripeptide groups are at least *quasispherical*.

The PMF can be considered as a solvent averaged potential surface along the reaction coordinate of an exchange reaction. Following Samoilov's concept of ion hydration[22,23] we characterise the activated jumps of a co-solvent i from an immediate vicinity of another co-solvent j by an activation energy E_{ij} which can be calculated from the corresponding PMF $F_{ij}(r)$ as:

$$E_{ij} = F_{ij}(r^1_{\max}) - F_{ij}(r^1_{\min}), \qquad (3)$$

where the $r^1_{\max}$ and $r^1_{\min}$ are the positions of the first maximum and minimum of the PMF. In all our calculations we calculate the PMF values with respect to the large r limit (zero as plotted). In such a model, the transition of a water molecule from the first to the second minimum of $F(r)$ is considered as an activated barrier crossing process.

Samoilov measured ion(I)–water(W) activation energies E_{IW} for different ions and compared them with the self-activation energy E_{WW} of water molecules associated with water–water interactions by calculating the difference, $\Delta E_{\mathrm{IW}} = E_{\mathrm{IW}} - E_{\mathrm{WW}}$. He introduced terms 'negative hydration' corresponding to the case $\Delta E_{\mathrm{IW}} < 0$ and 'positive hydration' for $\Delta E_{\mathrm{IW}} > 0$. Negative hydration is commonly associated with a local disruption of water structure in the vicinity of a hydrated ion. Positive hydration is associated with more structured water in the vicinity of a hydrated ion.[22,23,39] This is why the negatively hydrated ions are usually called 'chaotropes', and the positively hydrated ions—'kosmotropes'. A good estimate of E_{WW} is the activation energy of the hydrogen bonding site pair (water oxygen–water hydrogen), E_{OH},[3] which we will use in this paper.

We note that in his original paper, Samoilov measured the activation energies for individual ions from experimental data of self-diffusion of water and of the temperature coefficients of the ion mobilities in solution. Indeed, transition state theory[3] tells us that the activation energy ΔE_{IW} and the average residence time of water molecules in the vicinity of an ion τ_{IW} are related *via* the rather simple formula:

$$\tau_{\mathrm{IW}} = \frac{k_{\mathrm{B}}T}{h}\exp\left(\frac{\Delta E_{\mathrm{IW}}}{k_{\mathrm{B}}T}\right). \qquad (4)$$

Therefore, one may conclude that the PMFs contain not only the static/structural information about water structure around the interaction sites but they also provide us with important information about the dynamics of water molecules in the vicinity of the hydrated groups (ions). In our opinion this makes them very useful for investigations of the co-solute–water interactions and macromolecule hydration. However, one should use the approximation (4) with care because it does not take into account the solvent reorganisation dynamics.[48,49] More complex multidimensional transition path sampling theory[50] gives better

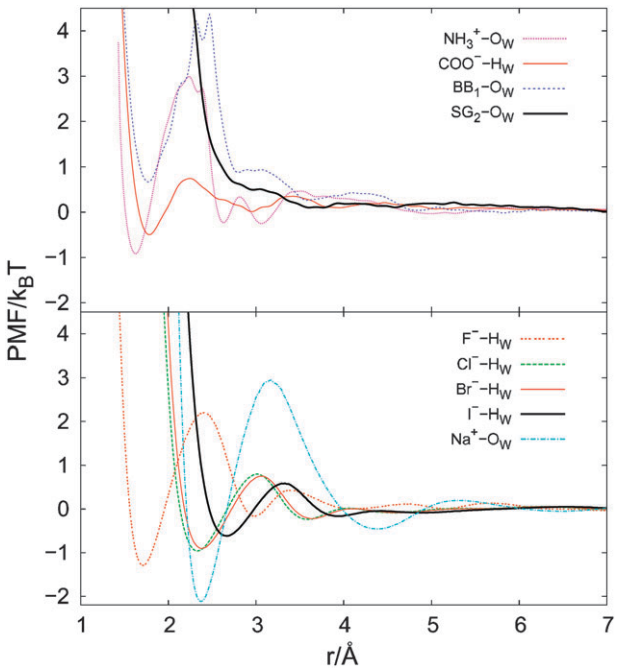

Fig. 7 PMFs between different tripeptide groups and water sites in bulk water solution are shown in the upper diagram. PMFs between ions and water sites in 1.0 M solution are shown in the lower diagram. The different lines are indicated on the corresponding legends. We characterize here the solute–water interactions of a cationic solute (NH_3^+ and Na^+) by the solute–water oxygen PMFs. For BB_1 and SG_2 groups we used the solute–water oxygen PMFs as well. For anionic solutes (COO^- and all investigated anions) we used the solute–water hydrogen PMFs.

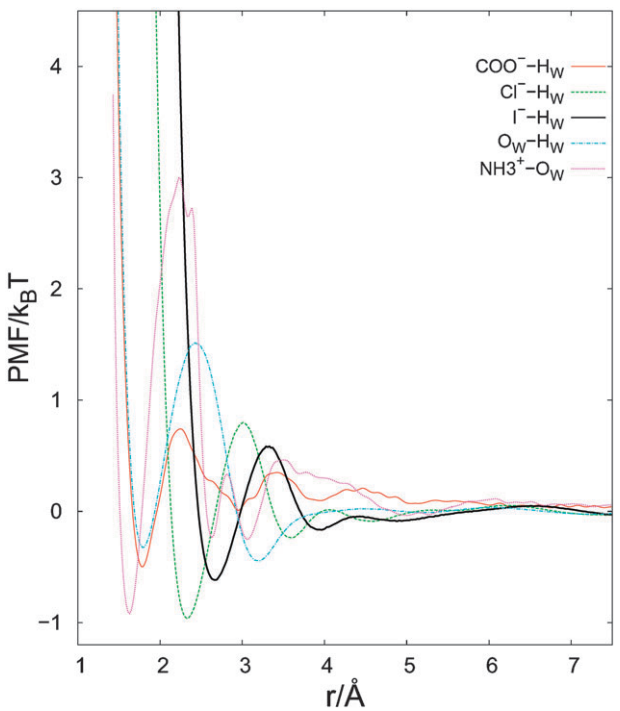

Fig. 8 PMFs corresponding to the water–water (oxygen–hydrogen PMF), chloride–water and peptide–water interactions for the charged sites of the trialanine polypeptide (NH_3^+ and COO^-).

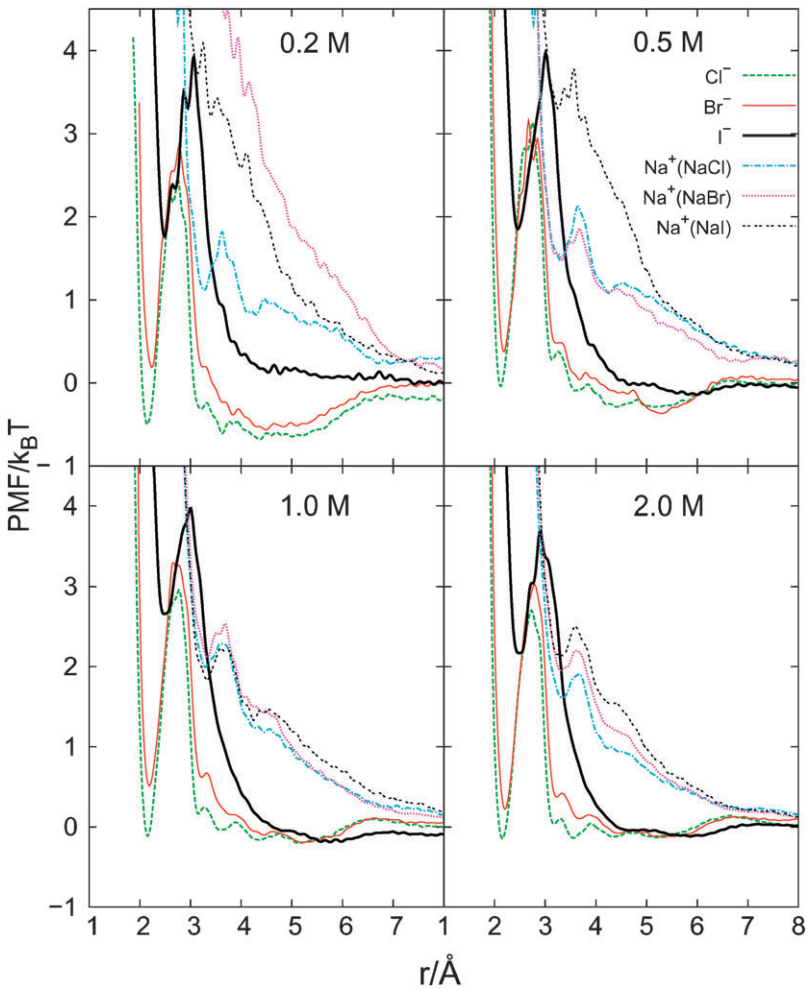

Fig. 9 NH_3^+ –ion PMFs. The different lines correspond to different ions as indicated on the corresponding legends. Different subplots correspond to different concentrations.

results, but we provide here the elementary formula (4) for the sake of simplicity.

In the following Fig. 7–12 we present the PMFs between water, ions and several tripeptide groups, namely: carboxyl terminus (COO^-), amino terminus (NH_3^+), first backbone group (BB_1) and second side chain group (SG_2). As the DCFs between the whole peptide and its co-solvents are oversmoothed by the orientational averaging we do not present here the PMFs for the whole peptide. The first, second and subsequent minima of the PMFs correspond to the maximum density of water sites in the corresponding water shells as a consequence of the PMF definition.

1. Peptide–water and ion–water interactions. In this section we present the peptide–water PMFs for bulk water solution and ion–water PMFs for 1.0 M solution. We characterise the solute–water interactions of a cationic solute (NH_3^+ and Na^+) by the solute–water oxygen PMFs. For BB_1 and SG_2 groups we used the solute–water oxygen PMFs as well. For anionic solutes (COO^- and all investigated anions) we used the solute–water hydrogen PMFs as the more relevant ones.

The PMFs for the tripeptide groups are shown in the top part of Fig. 7. The ion–water PMFs are shown at the bottom of this figure. For comparison, we plotted the water oxygen–hydrogen PMF together with selected ion–water and peptide–water PMFs in a separate figure, Fig. 8.

The activation energy E_{OH} obtained for bulk TIP5P-EW water is 1.8 k_BT (see Fig. 8). One can see from the PMFs presented in Fig. 7 that NH_3^+ ($E_{NH_3O} = 3.9\ k_BT$), Na^+ ($E_{NaO} = 5.1\ k_BT$) and F^- ($E_{FH} = 3.4\ k_BT$) are positively hydrated; COO^- ($E_{(COO)H} = 1.2\ k_BT$) and I^- ($E_{IH} = 1.2\ k_BT$) are negatively hydrated; Cl^- ($E_{ClH} = 1.8\ k_BT$) and Br^- ($E_{BrH} = 1.7\ k_BT$) have an activation energy not very different from that of bulk water. The obtained values of activation energies for sodium and halide ions and the character of their hydration (positive or negative) are in good correspondence with other theoretical and experimental investigations of monoatomic ion hydration.[3,22,23,39,43] The results for NH_3^+ and COO^- groups are also in line with recent computational

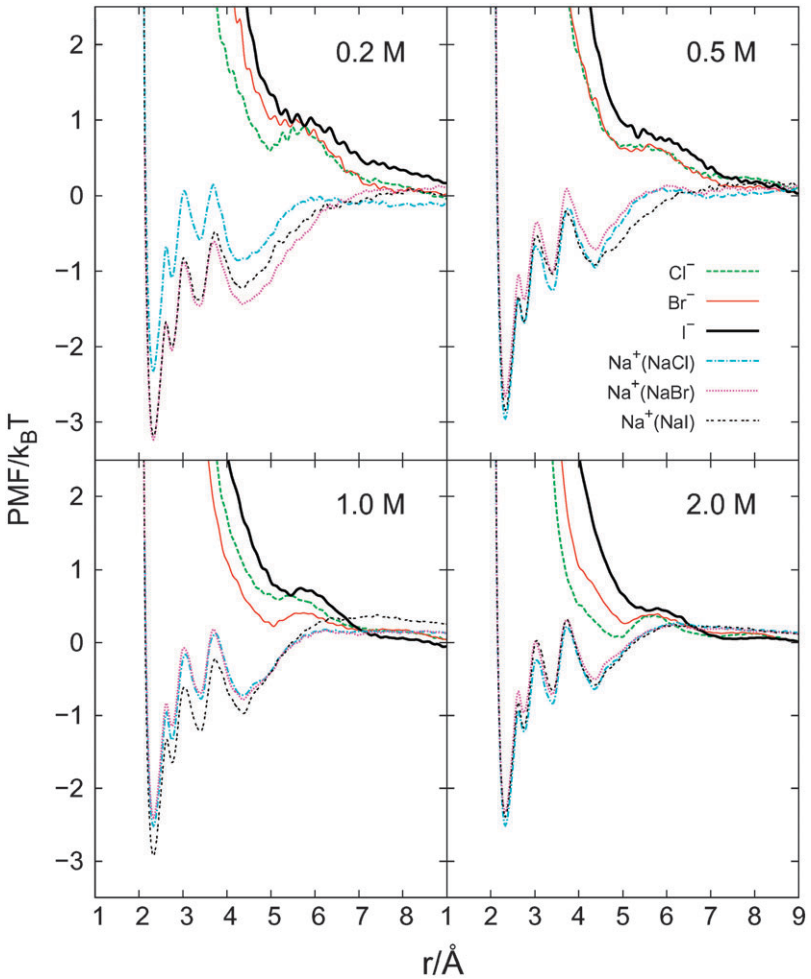

Fig. 10 The same data as Fig. 9 for the carboxyl terminus (COO^-) of the tripeptide.

and experimental studies on hydration of different charged biomolecule groups.[51–54]

The PMF of the hydrophobic group SG_2 does not have any pronounced extrema because of the effective depletion of water density around hydrophobic solutes. The results for the BB_1 group are somewhat peculiar: on one hand, the PMF value corresponding to the first minimum is positive, $F(r_{min}) \simeq 0.7\ k_BT$ which means that water molecules prefer to stay away from this group (one can see from Fig. 7 that the form of BB_1 PMF is very similar to the PMF of the hydrophobic SG_2 group for $r > 2.5$ Å). On the other hand, the activation energy for this group is twice the value calculated for E_{OH} ($E_{BB_1O} = 3.7\ k_BT$), which is evidence of positive hydration. Such behaviour is a consequence of the large dipole moment of the BB_1 group and the geometrical constraints. So, there is an effective depletion of water density around this group because it has a relatively small solvent accessible surface, but the water molecules which approach the BB_1 close enough can be 'trapped' by the short-range dipole–dipole interactions with the BB_1 dipole. These results are in good agreement with recent theoretical and experimental studies on peptide hydration[55,56] where it was shown that the water molecules interact much more strongly with the backbone groups than with the non-polar side-chain groups.

2. NH_3^+-ion interactions. We present NH_3^+-ion PMFs in Fig. 9. One can see from this figure that only Cl^- PMFs have slightly negative values ($\lesssim 0.0\ k_BT$) at the position of the first minimum. This means that for bigger anions the direct binding is less favourable than shell–shell contacts (see the secondary minima corresponding to the intersolute distance $\simeq$ 5–6 Å). This is especially true for the I^- ions for which $F(r_{min})$ obtains quite high positive values ($\gtrsim 2\ k_BT$). This is a consequence of the strong hydration of the NH_3^+ group (see above). There is a high energetic barrier for moving water molecules away from this group. Therefore, in spite of the attractive electrostatic interactions, big anions prefer to interact with this group by the shell–shell interactions (which correspond to the second minima on the plots) rather than by direct binding.

Because of the strong reorientation of water molecules around NH_3^+, there is a weak attraction between the NH_3^+ water shell and Na^+ ions which manifests itself in the slight minima in the Na^+–water PMFs around an intersolute distance of $r \sim 3.5$ Å.

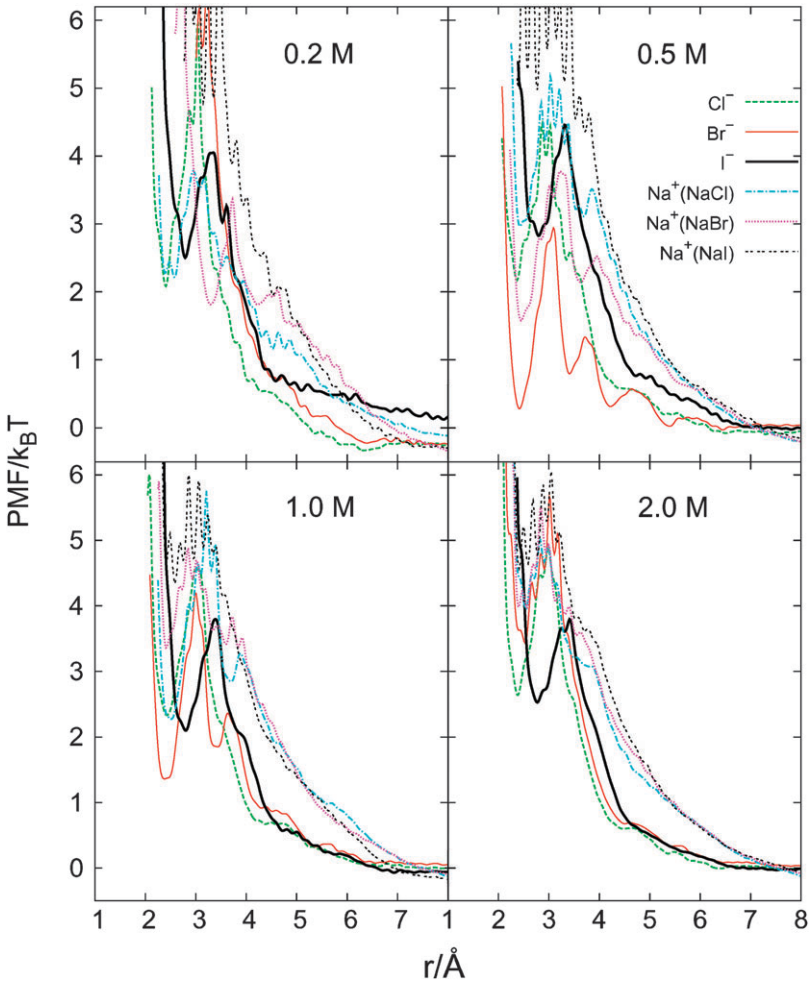

Fig. 11 The same data as in Fig. 9 for the first backbone group (BB_1) of the tripeptide.

3. COO^--ion interactions. The COO^- ion PMFs are shown in Fig. 10. Unlike the NH_3^+ group, the carboxylate terminus is relatively weakly hydrated (see Fig. 8) and the Na^+ cations easily move water molecules away—this group is surrounded by a cloud of sodium ions which are in direct contact with it. This cloud of positive charges slightly screens the repulsive COO^--anion interactions. As a consequence, some of the COO^--anion PMFs have noticeable minima around 4–5 Å. As the Na^+ are strongly hydrated, shell–shell and shell–group interactions also take place, as can be seen from the number of secondary minima on the corresponding PMFs. However, the COO^-–sodium interactions *via* intermediate water are less favourable than the direct COO^-–sodium contacts as can be seen from the large negative difference ($\sim$1–2 k_BT) between the depths of the first and secondary minima in the COO^-–Na^+ PMFs.

4. BB_1-ion interactions. The shapes of BB_1–ion PMFs presented in Fig. 11 are similar to those obtained for bulk water solution. There are more or less deep minima corresponding to the direct BB_1-ion contacts but with positive values of PMF(r_{min}). The activation energies of removing ions from this group are different for different solutions. Thus, the activation energies for Cl^- and Br^- anions are in the range $\sim$2–3 k_BT which is higher than E_{OH}. The activation energies of sodium cation vary in the range $\sim$1.5–2.5 k_BT which is close to the E_{OH} value 1.8 k_BT. The activation energies for I^- are in the range $\sim$1.1–1.7 k_BT which is slightly less than E_{OH}. At the same time, all these values are significantly less than the activation energy of removing water molecules from the BB_1 group (see above). Because of this, the values of $F(r_{min})$ are higher than 2 k_BT for most of the ions except for the Br^- in 0.5 and 1.0 M solutions.

5. SG_2-ion interactions. In Fig. 12 we present the PMFs corresponding to SG_2-ion interactions. All ions are repelled from this group because the ion–water interactions are stronger than the SG_2-ion interactions. For high concentrations ($\geq$ 0.5 M) and short intersolute distances ($r \sim$ 3–5 Å) this repulsion is smaller for anions than for cations, presumably because of the lower entropic gain from removing anions which are of bigger size than Na^+ (see ref. 57 and 58 for an explanation of this phenomenon).

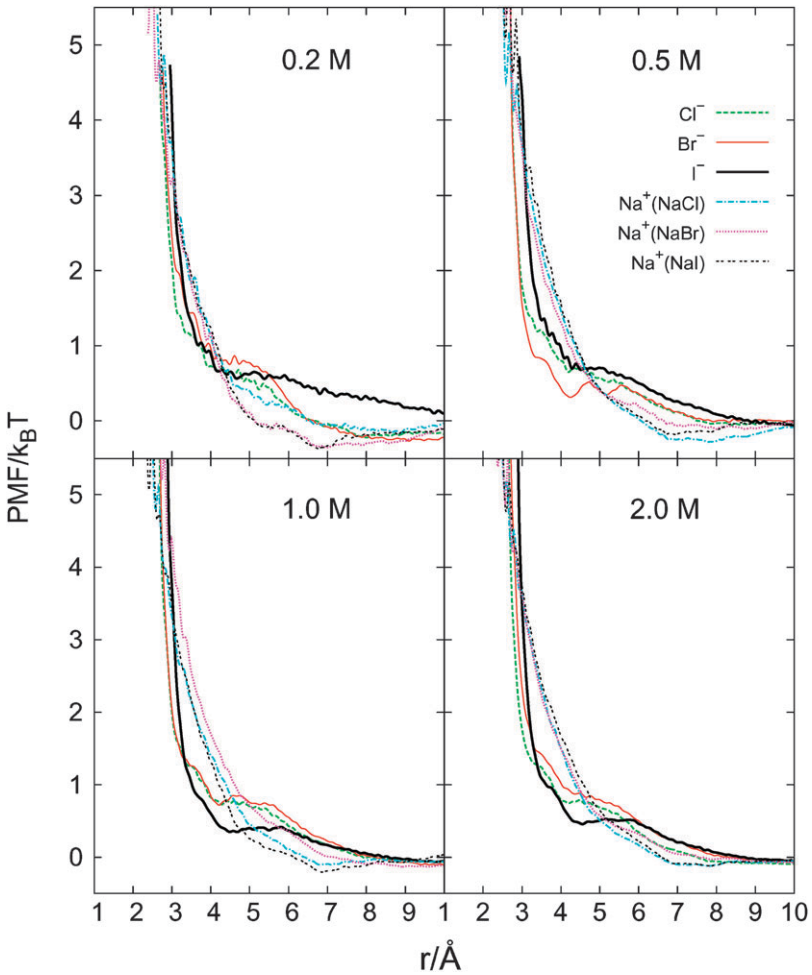

Fig. 12 The same data as Fig. 9 for the second side group (SG_2) of the tripeptide.

4. Conclusion

In this article, we have presented the results from MD simulations of the alanine tripeptide in different electrolyte solutions. Analysis of the results leads to the following conclusions:

1. Generally, the ions prefer contacts with peptide *via* intermediate water shell—the ion concentrations in the second solvation shell are significantly higher than in the first shell. The only exception is the case of the strong electrostatic attraction like the sodium–carboxyl group contacts or fluoride–amino group contacts. But for the larger ions the ion–water–peptide contacts are preferred to ion–peptide contacts.

2. In cases of comparatively small ionic radius (sodium cations, fluorine and chlorine anions), the ions tend to be attracted to highly charged groups (NH_3^+ and COO^- groups in our example). In the case of the bigger anions, both anions and cations tend to be closer to the hydrophobic peptide groups. This fact corresponds to the idea of 'quasi-hydrophobic' behaviour of the large halides.[57]

3. The chaotropes (bromide and iodide ions) tend to be close to the hydrophobic groups but the kosmotropes (fluoride and sodium ions) tend to be close to the hydrophilic groups. The chloride ions are almost 'neutral' in this sense, and they behave differently depending on the concentration. Taking into account different geometrical limits, this leads to a nonlinear effect of the anions on the tripeptide conformation which decreases with salt concentration.

4. The positively charged N-terminus is hydrated more strongly than the negatively charged C-terminus. This leads to quite different pictures of counterion interactions with these groups. There is a high energetic cost for moving water molecules away from the NH_3^+ group, and as a consequence, more weakly hydrated anions prefer to interact with that group *via* an intermediate water shell rather than by the direct contacts. This is especially true for the most chaotropic ion in our study, I^-, which has a large positive difference ($\gtrsim 2\ k_BT$) between the depths of the first and secondary NH_3^+–I^- PMF minima. In contrast, the direct contact interactions between the negatively hydrated COO^- group and positively hydrated sodium cations are more favourable than the sodium–COO^- contacts *via* intermediate water.

The hypotheses of preferential ion exclusion from the protein–water interface[20] has to be revisited by forthcoming combined theoretical and computational studies. As one may see from these current results and from the experimental data[10–12] the net effect of salts on polypeptides depends on the polypeptide primary structure and the particular

conditions of ionic solution (concentration, sort of ions, *etc*.). In principle, all the above described effects (Debye–Hückel screening, electroselectivity and Hofmeister effects) are important and we can neglect none of them *a priori*.

We have shown in this article that classical molecular dynamics with a non-polarisable force-field is able to qualitatively reproduce most of the important effects of macromolecule hydration in electrolyte solutions. Nevertheless, to improve the predictive power of the molecular simulations, one has to use more advanced methods of quantum chemistry to take into account such important effects as the influence of ions on the proton exchange *via* peptide groups and water molecules and the polarisation of big ions and water molecules. As these methods are computationally too expensive to model macromolecules in bulk electrolyte solutions, a reasonable compromise could be the hybrid QM/MM methods where different subsystems are treated simultaneously on a different level of approximation.

We believe that the forthcoming study of bigger polypeptide complexes with large-scale molecular dynamics and QM/MM simulations will shed further light on this intriguing problem. We also think that these results could provoke new experimental studies in this area.

Acknowledgements

We acknowledge the financial support provided by the Unilever company and the supercomputer facilities provided by the Irish Centre for High-End Computing (ICHEC), Dublin. We are grateful to Robert Glen, Dmitry Nerukh, Gennady Chuev and Alexei Kornyshev for their critical comments. Our special thanks to Ruth Lynden-Bell for very useful discussions on different aspects of ion hydration.

References

1 *Water and Biological Macromolecules*, ed. E. Westhof, The Macmillan Press Ltd, 1993.
2 N. C. Price, R. A. Dwek, M. Wormald and G. R. Ratcliffe, *Principles and problems in physical chemistry for biochemists*, Oxford University Press, 2001.
3 *Molecular theory of solvation*, ed. F. Hirata, Kluwer Academic Publishers, Dordrecht, the Netherlands, 2003.
4 R. L. Baldwin, How Hofmeister ion interactions affect protein stability, *Biophys. J*., 1996, **71**(4), 2056–2063.
5 J. S. Perkyns, Y. Y. Wang and B. M. Pettitt, Salting in peptides, conformationally dependent solubilities and phase behavior of a tripeptide zwitterion in electrolyte solution, *J. Am. Chem. Soc*., 1996, **118**(5), 1164–1172.
6 S. A. Hassan, Amino acid side chain interactions in the presence of salts, *J. Phys. Chem. B*, 2005, **109**(46), 21989–21996.
7 T. Ghosh, A. Kalra and S. Garde, On the salt-induced stabilization of pair and many-body hydrophobic interactions, *J. Phys. Chem. B*, 2005, **109**(1), 642–651.
8 M. Kinoshita and Y. Harano, Potential of mean force between solute atoms in salt solution: Effects due to salt species and relevance to conformational transition of biomolecules, *Bull. Chem. Soc. Jpn*., 2005, **78**(8), 1431–1441.
9 T. Arakawa and S. N. Timasheff, Abnormal solubility behavior of beta-lactoglobulin salting-in by glycine and NaCl, *Biochemistry*, 1987, **26**(16), 5147–5153.
10 Y. Goto, N. Takahashi and A. L. Fink, Mechanism of acid-induced folding of proteins, *Biochemistry*, 1990, **29**, 3480–3488.
11 Y. Goto and S. Aimoto, Anion and pH-dependent conformational transition of an amphiphilic polypeptide, *J. Mol. Biol*., 1991, **218**(2), 387–396.
12 Y. Goto and Y. Hagihara, Mechanism of the conformational transition of melittin, *Biochemistry*, 1992, **31**(3), 732–738.
13 R. A. Curtis, J. M. Prausnitz and H. W. Blanch, Protein–protein and protein–salt interactions in aqueous protein solutions containing concentrated electrolytes, *Biotechnol. Bioeng*., 1998, **57**(1), 11–21.
14 R. A. Curtis, J. Ulrich, A. Montaser, J. M. Prausnitz and H. W. Blanch, Protein–protein interactions in concentrated electrolyte solutions—Hofmeister-series effects, *Biotechnol. Bioeng*., 2002, **79**(4), 367–380.
15 J. J. McManus, J. O. Radler and K. A. Dawson, Does calcium turn a zwitterionic lipid cationic?, *J. Phys. Chem. B*, 2003, **107**(36), 9869–9875.
16 J. J. McManus, J. O. Radler and K. A. Dawson, Observation of a rectangular columnar phase in a DNA–calcium–zwitterionic lipid complex, *J. Am. Chem. Soc*., 2004, **126**(49), 15966–15967.
17 M. C. Pinna, P. Bauduin, D. Touraud, M. Monduzzi, B. W. Ninham and W. Kunz, Hofmeister effects in biology: Effect of choline addition on the salt-induced super activity of horseradish peroxidase and its implication for salt resistance of plants, *J. Phys. Chem. B*, 2005, **109**(34), 16511–16514.
18 M. G. Cacace, E. M. Landau and J. J. Ramsden, The hofmeister series: salt and solvent effects on interfacial phenomena, *Q. Rev. Biophys*., 1997, **30**(3), 241–277.
19 G. Karlstrom, On the effective interaction between an ion and a hydrophobic particle in polar solvents, a step towards an understanding of the hofmeister effect?, *Phys. Chem. Chem. Phys*., 2003, **5**(15), 3238–3246.
20 S. N. Timasheff, Protein hydration, thermodynamic binding, and preferential hydration, *Biochemistry*, 2002, **41**(46), 13473–13482.
21 M. J. Blandamer, J. B. F. N. Engberts, P. T. Gleeson and J. C. R. Reis, Activity of water in aqueous systems; a frequently neglected property, *Chem. Soc. Rev*., 2005, **2005**, 440–458.
22 O. Ya. Samoilov, A new approach to the study of hydration of ions in aqueous solution, *Discuss. Faraday Soc*., 1957, 141–146.
23 *Structure of aqueous electrolyte solutions and the hydrationof ions*, ed. O. Ya. Samoilov, Consultants Bureau, New York, 1965..
24 H. J. C. Berendsen, D. van der Spoel and R. van Drunen, Gromacs: A message-passing parallel molecular dynamics implementation, *Comput. Phys. Commun*., 1995, **91**, 43–56.
25 E. Lindahl, B. Hess and D. van der Spoel, Gromacs 3.0: A package for molecular simulation and trajectory analysis, *J. Mol. Model*, 2001, **7**, 306–317.
26 G. A. Kaminski, R. A. Friesner, J. Tirado-Rives and W. L. Jorgensen, Evaluation and reparametrization of the OPLS-AA force field for proteins *via* comparison with accurate quantum chemical calculations on peptides, *J. Phys. Chem. B*, 2001, **105**(28), 6474–6487.
27 S. W. Rick, A reoptimization of the five-site water potential (tip5p) for use with ewald sums, *J. Chem. Phys*., 2004, **120**(13), 6085–6093.
28 M. W. Mahoney and W. L. Jorgensen, A five-site model for liquid water and the reproduction of the density anomaly by rigid, nonpolarizable potential functions, *J. Chem. Phys*., 2000, **112**(20), 8910–8922.
29 G. Schaftenaar and J. H. Noordik, Molden: a pre- and post-processing program for molecular and electronic structures, *J. Comput. Aided Mol. Des*., 2000, **14**, 123–134.
30 Y. G. Mu, D. S. Kosov and G. Stock, Conformational dynamics of trialanine in water, 2. comparison of AMBER, CHARM, GROMOS, and OPLS force fields to NMR and infrared experiments, *J. Phys. Chem. B*, 2003, **107**(21), 5064–5073.
31 M. V. Fedorov, S. Schumm and J. M. Goodman, Solvent effects and conformational stability of a tripeptide, *Lecture Notes Bioinf*., 2006, **4216**, 141–149, In the Proceedings of the Computational Life Sciences II.
32 S. Woutersen and P. Hamm, Structure determination of trialanine in water using polarization sensitive two-dimensional vibrational spectroscopy, *J. Phys. Chem. B*, 2000, **104**(47), 11316–11320.
33 S. Woutersen and P. Hamm, Isotope-edited two-dimensional vibrational spectroscopy of trialanine in aqueous solution, *J. Chem. Phys*., 2001, **114**(6), 2727–2737.

34 R. Schweitzer-Stenner, F. Eker, Q. Huang and K. Griebenow, Dihedral angles of trialanine in D2O determined by combining FTIR and polarized visible raman spectroscopy, *J. Am. Chem. Soc.*, 2001, **123**(39), 9628–9633.
35 D. van der Spoel and E. Lindahl, Brute-force molecular dynamics simulations of villin headpiece: Comparison with NMR parameters, *J. Phys. Chem. B*, 2003, **107**(40), 11178–11187.
36 H. J. C. Berendsen, J. P. M. Postma, W. F. van Gunsteren, A. Dinola and J. R. Haak, Molecular-dynamics with coupling to an external bath, *J. Chem. Phys.*, 1984, **81**(8), 3684–3690.
37 http://www.octave.org.
38 http://www.gnuplot.info.
39 Y. Marcus, *Ion solvation*, John Wiley & Sons, Chichester, UK, 1985.
40 *The Chemical Physics of Solvation, Part A*, eds. R. R. Dogonadze, E. Kalman, A. A. Kornyshev and J. Ulstrup, Elsevier, Amsterdam, 1985.
41 *The Chemical Physics of Solvation, Part B*, eds. R. R. Dogonadze, E. Kalman, A. A. Kornyshev and J. Ulstrup, Elsevier, Amsterdam, 1986.
42 *The Chemical Physics of Solvation, Part C*, eds. R. R. Dogonadze, E. Kalman, A. A. Kornyshev and J. Ulstrup, Elsevier, Amsterdam, 1988.
43 M. V. Fedorov and A. A. Kornyshev, Unravelling the solvent response to neutral and charged solutes, *Mol. Phys.*, 2007, **105**(1), 1–16.
44 A. Kalra, N. Tugcu, S. M. Cramer and S. Garde, Salting-in and salting-out of hydrophobic solutes in aqueous salt solutions, *J. Phys. Chem. B*, 2001, **105**(27), 6380–6386.
45 S. Pal and F. Muller-Plathe, Molecular dynamics simulation of aqueous NaF and NaI solutions near a hydrophobic surface, *J. Phys. Chem. B*, 2005, **109**(13), 6405–6415.
46 R. Zangi and B. J. Berne, Aggregation and dispersion of small hydrophobic particles in aqueous electrolyte solutions, *J. Phys. Chem. B*, 2006, **110**(45), 22736–22741.
47 R. Zangi, M. Hagen and B. J. Berne, Effect of ions on the hydrophobic interaction between two plates, *J. Am. Chem. Soc.*, 2007, **129**(15), 4678–4686.
48 P. L. Geissler, C. Dellago and D. Chandler, Kinetic pathways of ion pair dissociation in water, *J. Phys. Chem. B*, 1999, **103**(18), 3706–3710.
49 J. Marti, F. S. Csajka and D. Chandler, Stochastic transition pathways in the aqueous sodium chloride dissociation process, *Chem. Phys. Lett.*, 2000, **328**(1–2), 169–176.
50 P. G. Bolhuis, D. Chandler, C. Dellago and P. L. Geissler, Transition path sampling: Throwing ropes over rough mountain passes, in the dark, *Annu. Rev. Phys. Chem.*, 2002, **53**, 291–318.
51 S. Bandyopadhyay, S. Chakraborty and B. Bagchi, Secondary structure sensitivity of hydrogen bond lifetime dynamics in the protein hydration layer, *J. Am. Chem. Soc.*, 2005, **127**(47), 16660–16667.
52 S. Bandyopadhyay, S. Chakraborty, S. Balasubramanian and B. Bagchi, Sensitivity of polar solvation dynamics to the secondary structures of aqueous proteins and the role of surface exposure of the probe, *J. Am. Chem. Soc.*, 2005, **127**(11), 4071–4075.
53 S. Bandyopadhyay, S. Chakraborty and B. Bagchi, Exploration of the secondary structure specific differential solvation dynamics between the native and molten globule states of the protein HP-36, *J. Phys. Chem. B*, 2006, **110**(41), 20629–20634.
54 B. M. Messer, C. D. Cappa, J. D. Smith, W. S. Drisdell, C. P. Schwartz, R. C. Cohen and R. J. Saykally, Local hydration environments of amino acids and dipeptides studied by X-ray spectroscopy of liquid microjets, *J. Phys. Chem. B*, 2005, **109**(46), 21640–21646.
55 D. Russo, R. K. Murarka, G. Hura, E. Verschell, J. R. A. Copley and T. Head-Gordon, Evidence for anomalous hydration dynamics near a model hydrophobic peptide, *J. Phys. Chem. B*, 2004, **108**(51), 19885–19893.
56 D. Russo, R. K. Murarka, J. R. D. Copley and T. Head-Gordon, Molecular view of water dynamics near model peptides, *J. Phys. Chem. B*, 2005, **109**(26), 12966–12975.
57 R. M. Lynden-Bell and J. C. Rasaiah, From hydrophobic to hydrophilic behaviour: A simulation study of solvation entropy and free energy of simple solutes, *J. Chem. Phys.*, 1997, **107**(6), 1981–1991.
58 J. C. Rasaiah and R. M. Lynden-Bell, Computer simulation studies of the structure and dynamics of ions and non-polar solutes in water, *Philos. Trans. R. Soc. London, Ser. A*, 2001, **359**(1785), 1545–1574.